

# Synthesis, Structural Characterization, and Theoretical Investigation of Compounds Containing an Al–O–M–O–Al (M = Ti, Zr) Core<sup>†</sup>

Swadhin K. Mandal,<sup>‡</sup> Prabhuodeyara M. Gurubasavaraj,<sup>‡</sup> Herbert W. Roesky,<sup>\*,‡</sup> Rainer B. Oswald,<sup>§</sup> Jörg Magull,<sup>‡</sup> and Arne Ringe<sup>‡</sup>

*Institute of Inorganic Chemistry, University of Göttingen, Tammannstrasse 4, 37077 Göttingen, Germany, and Institute of Physical Chemistry, University of Göttingen, Tammannstrasse 6, 37077 Göttingen, Germany*

Received May 31, 2007

We report a facile route to the first molecular compounds with the Al–O–M–O–Al (M = Ti, Zr) structural motif. Synthesis of L(Me)Al( $\mu$ -O)M(NMe<sub>2</sub>)<sub>2</sub>( $\mu$ -O)Al(Me)L [L = CH{N(Ar)(CMe)}<sub>2</sub>, Ar = 2,6-*i*-Pr<sub>2</sub>C<sub>6</sub>H<sub>3</sub>; M = Ti (**7**), Zr (**8**)] was accomplished by reacting the monometallic hydroxide precursor L(Me)Al(OH) (**1**) with Ti(NMe<sub>2</sub>)<sub>4</sub> or Zr(NMe<sub>2</sub>)<sub>4</sub> under elimination of Me<sub>2</sub>NH in good yield. The crystal structural data confirm the trimetallic Al–O–M–O–Al core in both **7** and **8**. Preliminary investigation on catalytic activity of these complexes reveals low activity of these complexes in ethylene polymerization as compared to the related oxygen-bridged metallocene-based heterobimetallic complexes L(Me)Al( $\mu$ -O)M(Me)Cp<sub>2</sub> (M = Ti, Zr) which could be attributed to the relatively lower stability of the supposed cationic intermediate as revealed by DFT calculations.

## Introduction

Heterobi- and heteropolymetallic compounds are of significant interest ranging from advanced materials to valuable catalysts. The compounds with different metals have often modified the fundamental properties of the individual metal atoms.<sup>1</sup> This cooperative feature is difficult to achieve otherwise.<sup>2</sup> Moreover, the interest in metal and organometallic oxides stems not only from the application of these compounds in industry as catalysts or as cocatalysts but also as a model for the fixation of catalysts on oxide surfaces.<sup>3</sup> As a result, increasing attention has been focused on the synthesis and characterization of heterobimetallic oxides, which are used as polyfunctional catalysts and precursors for the preparation of bi- and polymetallic heterogeneous catalysts.<sup>4–7</sup> Appropriate proximity between two different

metals in a heterometallic complex would allow more pronounced chemical communication between the metals. Additionally, it is a synthetic challenge to assemble different metal centers of entirely different chemical properties into a single molecule.

We have recently reported the syntheses of a new class of heterometallic complexes (**3–6**, Chart 1) through oxygen bridging based on an Al–O–M motif, some of which are excellent candidates for homogeneous catalysis.<sup>8–12</sup> The synthetic strategy takes advantage of unprecedented syntheses of two monometallic hydroxide precursors, L(Me)Al(OH) (**1**)<sup>8</sup> [L = CH{N(Ar)(CMe)}<sub>2</sub>, Ar = 2,6-*i*-Pr<sub>2</sub>C<sub>6</sub>H<sub>3</sub>] and Cp\*<sub>2</sub>-

\* To whom correspondence should be addressed. E-mail: hroesky@wdg.de.

<sup>†</sup> Dedicated to Professor Roald Hoffmann on the occasion of his 70th birthday.

<sup>‡</sup> Institute of Inorganic Chemistry, University of Göttingen.

<sup>§</sup> Institute of Physical Chemistry, University of Göttingen.

(1) Ueland, B. G.; Lau, G. C.; Cava, R. J.; O'Brien, J. R.; Schiffer, P. *Phys. Rev. Lett.* **2006**, *96*, 027216.

(2) Tao, R.-J.; Li, F.-A.; Zang, S.-Q.; Cheng, Y.-X.; Wang, Q.-L.; Niu, J.-Y.; Liao, D.-Z. *J. Coord. Chem.* **2006**, *59*, 901–909.

(3) Copéret, C.; Chabanas, M.; Saint-Arroman, R. P.; Basset, J.-M. *Angew. Chem., Int. Ed.* **2003**, *42*, 156–181.

(4) Roesky, H. W.; Haiduc, I.; Hosmane, N. S. *Chem. Rev.* **2003**, *103*, 2579–2595.

(5) Carofoglio, T.; Floriani, C.; Rosi, M.; Chiesi-Villa, A.; Rizzoli, C. *Inorg. Chem.* **1991**, *30*, 3245–3246.

(6) Rau, M. S.; Kretz, C. M.; Geoffroy, G. L.; Rheingold, A. L.; Haggerty, B. S. *Organometallics* **1994**, *13*, 1624–1634.

(7) Li, H.; Eddaoudi, M.; Lévert, J.; O'Keeffe, M.; Yaghi, O. M. *J. Am. Chem. Soc.* **2000**, *122*, 12409–12410.

(8) Bai, G.; Singh, S.; Roesky, H. W.; Noltemeyer, M.; Schmidt, H.-G. *J. Am. Chem. Soc.* **2005**, *127*, 3449–3455.

(9) Chai, J.; Jancik, V.; Singh, S.; Zhu, H.; He, C.; Roesky, H. W.; Schmidt, H.-G.; Noltemeyer, M.; Hosmane, N. S. *J. Am. Chem. Soc.* **2005**, *127*, 7521–7528.

(10) Gurubasavaraj, P. M.; Mandal, S. K.; Roesky, H. W.; Oswald, R. B.; Pal, A.; Noltemeyer, M. *Inorg. Chem.* **2007**, *46*, 1056–1061.

(11) Singh, S.; Roesky, H. W. *Dalton Trans.* **2007**, 1360–1370.

(12) Nembenna, S.; Roesky, H. W.; Mandal, S. K.; Oswald, R. B.; Pal, A.; Herbst-Irmer, R.; Noltemeyer, M.; Schmidt, H.-G. *J. Am. Chem. Soc.* **2006**, *128*, 13056–13057.



M–O–Al (M = Ti, Zr) core was accomplished by reacting the monometallic hydroxide precursor, L(Me)Al(OH) (**1**), with sterically less crowded group 4 nonmetallocene precursor M(NMe<sub>2</sub>)<sub>4</sub> under elimination of Me<sub>2</sub>NH. Reaction of 2 equiv of **1** with an 1 equiv of M(NMe<sub>2</sub>)<sub>4</sub> (M = Zr, Ti) in toluene leads to the intermolecular elimination of Me<sub>2</sub>NH and the formation of the  $\mu$ -O-bridged trimetallic complex, L(Me)Al( $\mu$ -O)M(NMe<sub>2</sub>)<sub>2</sub>( $\mu$ -O)Al(Me)L [M = Ti (**7**), Zr (**8**)] (Scheme 1). The absence of the characteristic OH resonance of L(Me)Al(OH) (**1**) in the <sup>1</sup>H NMR spectrum of the reaction mixture indicates the complete consumption of **1** into **7** and **8**, respectively. These complexes (**7**, **8**) were characterized by <sup>1</sup>H and <sup>13</sup>C NMR spectroscopy, elemental analysis, EI mass spectrometry, and single-crystal X-ray diffraction studies. Both of these complexes are soluble in *n*-hexane, pentane, toluene, and benzene at room temperature. The <sup>1</sup>H NMR spectra of **7** and **8** feature a characteristic singlet each at  $\sim$ 2.8 ppm attributed to the –NMe<sub>2</sub> protons, and the Al–(Me) protons resonate at  $\sim$ –0.6 ppm as another singlet. The singlet at  $\sim$ 2.8 ppm integrates twice against the singlet at  $\sim$ –0.6 ppm revealing the formation of trimetallic complexes as formulated in Scheme 1. In addition, a set of resonances assignable to the protons associated with the  $\beta$ -diketiminato ligand (L) are found in the <sup>1</sup>H NMR spectra of **7** and **8**. The <sup>27</sup>Al NMR is silent due to the quadrupolar nuclei of aluminum. The <sup>13</sup>C NMR spectra of **7** and **8** respectively reveal a singlet ( $\sim$  –11.0 ppm) assigned to the aluminum-bound methyl–carbon resonance and another singlet ( $\sim$ 44.0 ppm) that could be assigned to the four methyl carbon resonances arising from the two dimethylamino groups attached to the Ti or Zr center. The mass spectral data for **7** are in accord with the assigned structure. It exhibits the molecular ion peak at *m/e* 1086.8, and the next peak for compound **7** was observed at *m/e* 1071.8 corresponding to [M – Me]<sup>+</sup>. However the mass spectrometry data for **8** are quite different from those of **7** revealing no characteristic fragment except the base peak at *m/e* 202, which can be assigned to [DippNCMe]<sup>+</sup>.<sup>14</sup> Analytically pure crystals of **7** and **8** were grown from pentane and *n*-hexane solution, respectively, and finally the structures of **7** and **8** were unambiguously determined by single-crystal X-ray crystallography.

**X-ray Crystal Structures of 7 and 8.** The yellow single crystals of **7** and colorless single crystals of **8** were analyzed by X-ray diffraction studies (Figures 1 and 2). Compound **7** was crystallized from pentane at –30 °C whereas complex **8** was crystallized from *n*-hexane at 0 °C. Table 1 lists the crystallographic data, and the important bond parameters are listed in Table 2. Compounds **7** and **8** crystallize in the monoclinic space group *P2<sub>1</sub>/c*. Both aluminum atoms are bonded through an oxygen atom to titanium (in **7**) and zirconium (in **8**), respectively, and contain a bent Al–O–M (M = Ti, Zr) core as revealed by the corresponding bond angles (Table 2). The aluminum atom exhibits a distorted tetrahedral geometry with two nitrogen atoms of the  $\beta$ -diketiminato ligand, a methyl group, and one ( $\mu$ -O) unit. The

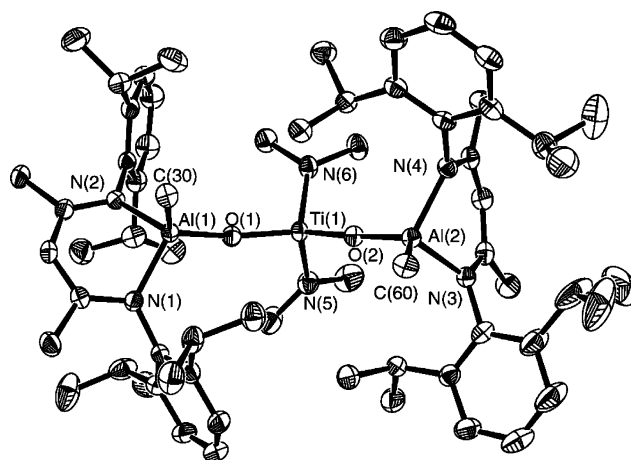


**Figure 1.** Molecular structure of **7** in the crystal (50% probability ellipsoids). Hydrogen atoms are omitted for clarity.

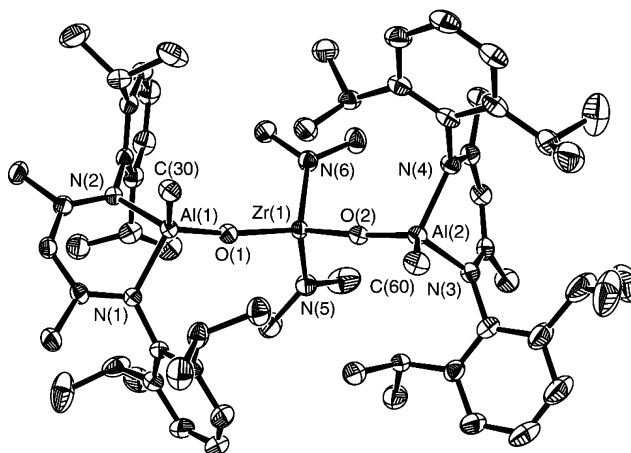


**Figure 2.** Molecular structure of **8** in the crystal (50% probability ellipsoids). Hydrogen atoms are omitted for clarity.

titanium or zirconium center also adopts a distorted tetrahedral geometry, and their coordination spheres are completed by two dimethylamino ligands and two ( $\mu$ -O) units. The Al–C(Me) bond length (average 1.96 Å in both **7** and **8**) compares very well to the recently structurally characterized oxygen-bridged heterobimetallic compounds of the general formula L(Me)Al( $\mu$ -O)M(R)Cp<sub>2</sub> (R = Me or Cl; M = Ti, Zr, or Hf).<sup>8,10</sup> The Al–( $\mu$ -O) bond length (average 1.73 Å in **7** and 1.72 Å in **8**) is in good agreement with that observed for L(Me)Al( $\mu$ -O)Ti(Me)Cp<sub>2</sub> (1.715(3) Å) and L(Me)Al( $\mu$ -O)Zr(R)Cp<sub>2</sub> (average 1.72 Å; R = Me or Cl) but longer than those found in compounds [(Me<sub>3</sub>Si)<sub>2</sub>HC]<sub>2</sub>Al<sub>2</sub>( $\mu$ -O) (1.687(4) Å)<sup>15</sup> and [HC{(CMe)(NMe)}<sub>2</sub>AlCl]<sub>2</sub>( $\mu$ -O) (1.677(6) Å).<sup>16</sup> The Ti–O bond distance in **7** (average 1.80 Å) and the Zr–O bond length in **8** (average 1.94 Å) are in good agreement with that observed for L(Me)Al( $\mu$ -O)Ti(Me)Cp<sub>2</sub> (1.808(3) Å)<sup>10</sup> and L(Me)Al( $\mu$ -O)Zr(R)Cp<sub>2</sub> (average 1.92 Å), respectively.<sup>8</sup> Two types of Al–O–M bond angles are noticed in both **7** and **8**. For example, one Al–O–M bond angle is almost linear (175.58(8)° in **7** and 173.21(10)° in **8**) while the other Al–O–M bond angle is

(15) Uhl, W.; Koch, M.; Hiller, W.; Heckel, M. *Angew. Chem.* **1995**, *107*, 1122–1124; *Angew. Chem., Int. Ed.* **1995**, *34*, 989–990.

(16) Kuhn, N.; Fuchs, S.; Niquet, E.; Richter, M.; Steimann, M. *Z. Anorg. Allg. Chem.* **2002**, *628*, 717–718.

(14) Prust, J.; Most, K.; Müller, I.; Alexopoulos, E.; Stasch, A.; Usón, I.; Roesky, H. W. *Z. Anorg. Allg. Chem.* **2001**, *627*, 2032–2037.

**Table 1.** Crystallographic and Structure Refinement Data for Compounds **7** and **8**

param	<b>7</b>	<b>8</b>
empirical formula	C <sub>64</sub> H <sub>100</sub> Al <sub>2</sub> N <sub>6</sub> O <sub>2</sub> Ti	C <sub>64</sub> H <sub>100</sub> Al <sub>2</sub> N <sub>6</sub> O <sub>2</sub> Zr
fw	1087.36	1130.68
<i>T</i> (K)	133(2)	133(2)
cryst system, space group	monoclinic, <i>P</i> 2 <sub>1</sub> / <i>c</i>	monoclinic, <i>P</i> 2 <sub>1</sub> / <i>c</i>
<i>a</i> (Å)	22.6235(9)	22.6139(9)
<i>b</i> (Å)	17.1285(4)	17.1826(8)
<i>c</i> (Å)	17.1933(5)	17.2375(6)
α (deg)	90	90
β (deg)	103.433(3)	102.419(3)
γ (deg)	90	90
<i>V</i> (Å <sup>3</sup> )	6480.2(4)	6541.2(5)
<i>Z</i>	4	4
abs coeff (mm <sup>-1</sup> )	0.204	0.239
<i>F</i> (000)	2360	2432
θ range for data collcn (deg)	1.51–24.84	1.50–24.90
no. of reflns collcd/unique	98 282/11 152 [R(int) = 0.0826]	66 342/11 255 [R(int) = 0.1005]
obsd reflns [ <i>I</i> > 2σ( <i>I</i> )]	8232	8169
data/restns/params	11 152/0/732	11 255/0/732
goof	0.966	0.967
R <sub>1</sub> , wR <sub>2</sub> [ <i>I</i> > 2σ( <i>I</i> )]	0.0395, 0.0910	0.0373, 0.0744
R <sub>1</sub> , wR <sub>2</sub> (all data)	0.0620, 0.0977	0.0647, 0.0810
largest diff peak/hole (e Å <sup>-3</sup> )	0.342 and -0.353	0.243 and -0.321

**Table 2.** Selected Bond Distances (Å) and Angles (deg) for Compounds **7** and **8**

Compound <b>7</b>			
Ti(1)–O(1)	1.798(1)	Ti(1)–O(2)	1.809(1)
Ti(1)–N(5)	1.923(2)	Ti(1)–N(6)	1.910(2)
Al(1)–O(1)	1.725(1)	Al(1)–N(1)	1.916(2)
Al(1)–N(2)	1.936(2)	Al(1)–C(30)	1.965(2)
Al(2)–O(2)	1.734(2)	Al(2)–N(3)	1.908(2)
Al(2)–N(4)	1.926(2)	Al(2)–C(60)	1.950(2)
O(1)–Ti(1)–O(2)	119.58(6)	O(1)–Ti(1)–N(6)	108.55(7)
O(2)–Ti(1)–N(6)	106.35(7)	O(1)–Ti(1)–N(5)	106.61(7)
O(2)–Ti(1)–N(5)	109.64(7)	N(6)–Ti(1)–N(5)	105.24(7)
Al(1)–O(1)–Ti(1)	166.18(9)	Al(2)–O(2)–Ti(1)	175.58(8)
O(1)–Al(1)–N(1)	113.34(7)	O(1)–Al(1)–N(2)	113.68(7)
N(1)–Al(1)–N(2)	94.97(7)	O(1)–Al(1)–C(30)	116.96(8)
N(1)–Al(1)–C(30)	108.46(8)	N(2)–Al(1)–C(30)	107.08(8)
O(2)–Al(2)–N(3)	108.22(7)	O(2)–Al(2)–N(4)	107.85(7)
N(3)–Al(2)–N(4)	95.32(7)	O(2)–Al(2)–C(60)	119.24(8)
N(3)–Al(2)–C(60)	110.00(9)	N(4)–Al(2)–C(60)	113.49(8)
Compound <b>8</b>			
Zr(1)–O(1)	1.941(2)	Zr(1)–O(2)	1.944(2)
Zr(1)–N(5)	2.072(2)	Zr(1)–N(6)	2.057(2)
Al(1)–O(1)	1.716(2)	Al(1)–N(1)	1.913(2)
Al(1)–N(2)	1.926(2)	Al(1)–C(30)	1.974(2)
Al(2)–O(2)	1.723(2)	Al(2)–N(3)	1.907(2)
Al(2)–N(4)	1.926(2)	Al(2)–C(60)	1.955(3)
O(1)–Zr(1)–O(2)	117.05(7)	O(1)–Zr(1)–N(6)	109.09(7)
O(2)–Zr(1)–N(6)	107.07(7)	O(1)–Zr(1)–N(5)	107.87(7)
O(2)–Zr(1)–N(5)	110.21(8)	N(6)–Zr(1)–N(5)	104.88(8)
Al(1)–O(1)–Zr(1)	166.50(10)	Al(2)–O(2)–Zr(1)	173.21(10)
O(1)–Al(1)–N(1)	112.86(8)	O(1)–Al(1)–N(2)	112.98(8)
N(1)–Al(1)–N(2)	95.20(9)	O(1)–Al(1)–C(30)	117.65(10)
N(1)–Al(1)–C(30)	108.81(10)	N(2)–Al(1)–C(30)	106.92(10)
O(2)–Al(2)–N(3)	107.74(8)	O(2)–Al(2)–N(4)	107.56(9)
N(3)–Al(2)–N(4)	95.20(9)	O(2)–Al(2)–C(60)	119.15(10)
N(3)–Al(2)–C(60)	110.60(11)	N(4)–Al(2)–C(60)	113.83(10)

slightly bent (166.18(9)° in **7** and 166.50(10)° in **8**). These bond angles sharply contrast to the Al–O–M bond angle observed in the heterobimetallic complexes, L(Me)Al(μ-O)–Ti(Me)Cp<sub>2</sub> (151.7(2)°)<sup>10</sup> and L(Me)Al(μ-O)Zr(R)Cp<sub>2</sub> (average 156.8°)<sup>8</sup> or the recently characterized trimetallic complex L(Me)Al(μ-O)Mg(THF)<sub>2</sub>(μ-O)Al(Me)L (average 154.9°)<sup>12</sup> though these values compare well with that observed for the homobimetallic angle, M–(μ-O)–M (M = Zr, Hf), observed

in (Cp<sub>2</sub>ZrMe)<sub>2</sub>(μ-O) (174.1(3)°)<sup>17</sup> and (Cp<sub>2</sub>HfMe)<sub>2</sub>(μ-O) (173.9(3)°).<sup>18</sup>

### Ethylene Polymerization and Computational Studies.

Preliminary experiments were carried out for ethylene polymerization using compounds **7** and **8**, respectively, as precatalyst in the presence of methylalumoxane (MAO) as cocatalyst. The results reveal two orders lower activity in magnitude (on the order of 10<sup>4</sup> with MAO to catalyst ratio 800:1, activity = g of PE/(mol of catal·h)) even at relatively higher MAO to catalyst ratio, when compared to the activity observed in ethylene polymerization with metallocene-based heterobimetallic complexes [L(Me)Al(μ-O)M(Me)Cp<sub>2</sub> (M = Ti, Zr) bearing the Al–O–M moiety, **4**, Chart 1] reported from our laboratory.<sup>8,10</sup> This relatively lower activity in this study might be attributed to the lower stability of the supposed coordinatively unsaturated cationic intermediate of **7** or **8**. Density functional calculations were carried out to understand the bonding situation and the catalytic properties of compounds **7** and **8** and compare them to the related metallocene-based heterobimetallic complexes L(Me)Al(μ-O)Ti(Me)Cp<sub>2</sub> bearing the Al–O–Ti motif. As shown in Table 3, the calculated equilibrium structure matches very well with the data obtained by X-ray diffraction, thus giving a solid foundation for the electronic structure calculations to obtain further insight by investigating the molecular orbitals and bonds.

The bonding situation ascertained from the calculation predicts that generating a cation from **7** or **8** is more difficult as compared to that from the highly active catalyst L(Me)–Al(μ-O)Ti(Me)Cp<sub>2</sub> in which a cation is easily formed and stabilized by the Cp ligands. The examination of the bonds formed between the metal centers of **7** (Ti) or **8** (Zr) and oxygen clearly explains this behavior. The M–O bonds for both compounds are composed of a sd-hybrid orbital on the

(17) Hunter, W. E.; Hrcncir, D. C.; Bynum, R. V.; Penttila, R. A.; Atwood, J. L. *Organometallics* **1983**, *2*, 750–755.

(18) Fronczek, F. R.; Baker, E. C.; Sharp, P. R.; Raymond, K. N.; Alt, H. G.; Rausch, M. D. *Inorg. Chem.* **1976**, *15*, 2284–2289.

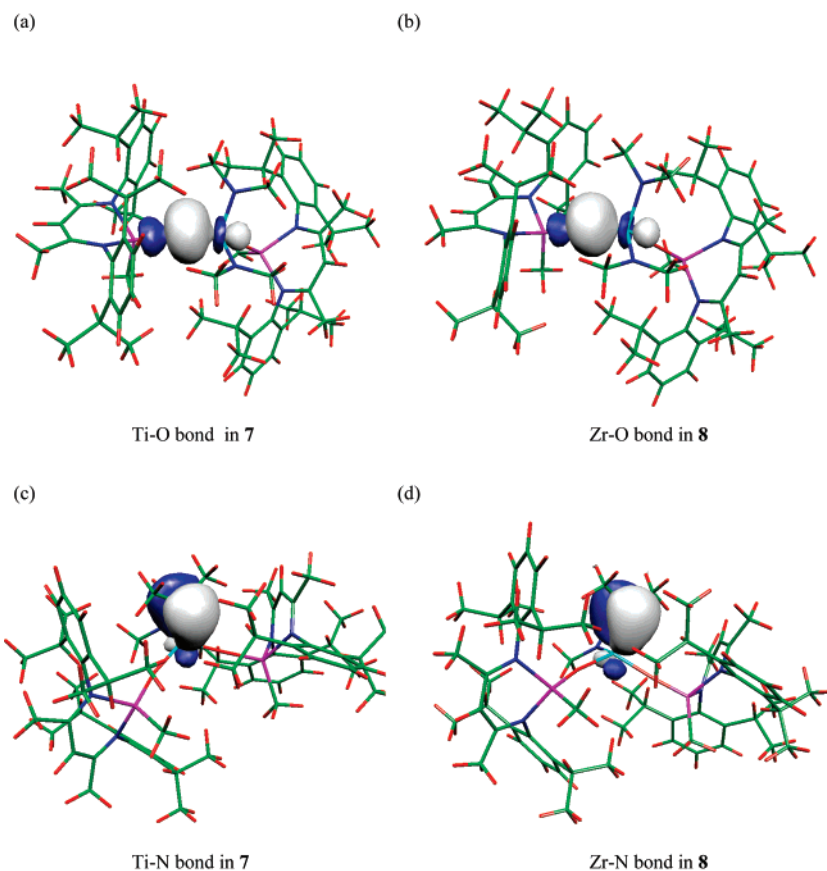


**Figure 3.** Shape of the bonding orbital around the metal center in **7** and **8**: (a) between Ti and oxygen; (b) between Zr and oxygen; (c) between Ti and nitrogen of dimethyl amino ligand; (d) between Zr and nitrogen of dimethyl amino ligand.

**Table 3.** Selected Calculated and X-ray Bond Distances (Å) and Bond Angles (deg) in **7** and **8**

bond dists	calcd	X-ray	bond angles	calcd	X-ray
Compound <b>7</b>					
Ti(1)–O(1)	1.809	1.798	O(1)–Ti(1)–N(6)	109.37	108.55
Ti(1)–O(2)	1.817	1.809	O(2)–Ti(1)–N(5)	110.23	109.64
Ti(1)–N(5)	1.928	1.923	O(1)–Ti(1)–O(2)	119.81	119.58
Ti(1)–N(6)	1.921	1.910	N(1)–Al(1)–N(2)	95.16	94.97
Compound <b>8</b>					
Zr(1)–O(1)	1.975	1.941	O(1)–Zr(1)–N(6)	109.87	109.09
Zr(1)–O(2)	1.984	1.944	O(2)–Zr(1)–N(5)	111.27	110.21
Zr(1)–N(5)	2.095	2.072	O(1)–Zr(1)–O(2)	118.60	117.05
Zr(1)–N(6)	2.087	2.057	N(1)–Al(1)–N(2)	95.08	95.20

metal with a nearly pure p-orbital from oxygen. The M–N bonds are formed as a result of overlap between the sd-hybrid orbital on the metal and the sp<sup>1.7</sup>-hybrid orbital on the nitrogen. The electronic density of both M–O and M–N bonds are primarily located on the O and N, respectively, leaving the metal center Lewis acidic (Figure 3). The situation is somewhat similar when the bonding in L(Me)–Al( $\mu$ -O)Ti(Me)Cp<sub>2</sub> is considered.<sup>10</sup> Interestingly, the stabilization of the M–O and M–N bonds occurs by means of a strong synergistic donor acceptor interaction between the bonding and antibonding orbitals among themselves stabilizing each of the bonds by about 15 kcal/mol. The formation of a cation results in disruption of this mutual synergy between these bonds around the Ti (Zr) center. Moreover, the enhanced Lewis acidity of the Ti (Zr) center of **7** (**8**) does not encourage the cation formation as easily as observed for L(Me)Al( $\mu$ -O)Ti(Me)Cp<sub>2</sub> in which the Cp ligand acts as

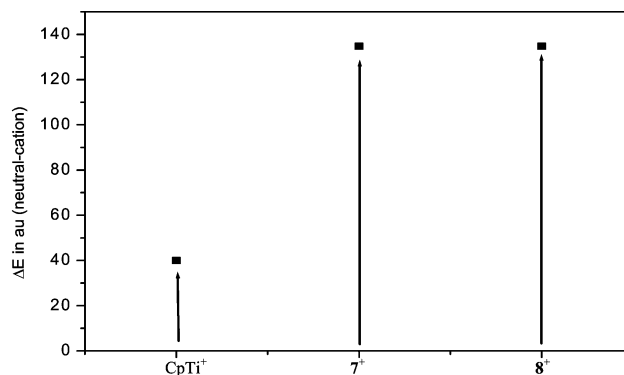


**Figure 4.** Relative energy needed to generate cationic species revealing that generation of the corresponding cation of **7** or **8** is more difficult than that of L(Me)Al( $\mu$ -O)Ti(Me)Cp<sub>2</sub> (CpTi<sup>+</sup>).

electronic buffer transferring necessary electron density to the metal center in the corresponding cation. This is also evident from the thermodynamic data revealing that the related energy needed to generate the corresponding cation of **7** (**8**) is more than three times that required to generate a cation from L(Me)Al( $\mu$ -O)Ti(Me)Cp<sub>2</sub> (Figure 4).

### Summary and Conclusion

In this contribution, we report the syntheses, characterization, and theoretical investigation of two covalently linked oxygen-bridged trimetallic complexes bearing the Al–O–M–O–Al (M = Ti, Zr) core. The synthetic strategy takes advantage of the recently synthesized kinetically stable

$L(\text{Me})\text{Al}(\text{OH})$  (**1**) [ $L = \text{CH}\{\text{N}(\text{Ar})(\text{CMe})\}_2$ ,  $\text{Ar} = 2,6\text{-}i\text{Pr}_2\text{C}_6\text{H}_3$ ] precursor as the building block. The Brønsted acidic character of the proton in the  $\text{Al}(\text{O}-\text{H})$  moiety allows almost clean reaction with less sterically hindered group 4 metal precursor  $\text{M}(\text{NMe}_2)_4$  ( $\text{M} = \text{Ti}, \text{Zr}$ ) forming compounds with the trimetallic core. Preliminary investigation on the catalytic activity reveals that these complexes exhibit low activity in ethylene polymerization as compared to the oxygen-bridged metallocene-based heterobimetallic complexes  $L(\text{Me})\text{Al}(\mu\text{-O})\text{M}(\text{Me})\text{Cp}_2$  ( $\text{M} = \text{Ti}, \text{Zr}$ ), which could be attributed to the relatively lower stability of the supposed cationic intermediate as revealed by DFT calculations.

## Experimental Section

**General Comments.** All experimental manipulations were carried out under an atmosphere of dry argon using standard Schlenk techniques. The samples for spectral measurements were prepared in a glovebox. The solvents were purified according to conventional procedures and were freshly distilled prior to use.  $\text{Ti}(\text{NMe}_2)_4$  (Alfa Aesar) and  $\text{Zr}(\text{NMe}_2)_4$  (Aldrich) were purchased from commercial sources and used without further purification.  $L(\text{Me})\text{Al}(\text{OH})$  (**1**) [ $L = \text{CH}\{\text{N}(\text{Ar})(\text{CMe})\}_2$ ,  $\text{Ar} = 2,6\text{-}i\text{Pr}_2\text{C}_6\text{H}_3$ ] was prepared by following the literature procedure.<sup>8</sup> NMR spectra were recorded on a Bruker Avance 500 instrument, and the chemical shifts downfield from the reference standard tetramethylsilane (TMS) were assigned positive values. Mass spectra were obtained on a Finnigan MAT 8230 spectrometer by the EI technique. Melting points were obtained in sealed capillaries on a Büchi B 540 instrument. Elemental analyses were performed at the Analytical Laboratory of the Institute of Inorganic Chemistry at Göttingen, Germany.

**Synthesis of  $L(\text{Me})\text{Al}(\mu\text{-O})\text{Ti}(\text{NMe}_2)_2(\mu\text{-O})\text{Al}(\text{Me})\text{L}$  (**7**).** A solution of  $L(\text{Me})\text{Al}(\text{OH})$  (0.477 g, 1.0 mmol) in toluene (20 mL) was added dropwise by a syringe over a period of 15 min to a solution of  $\text{Ti}(\text{NMe}_2)_4$  (0.112 g, 0.50 mmol) in toluene (20 mL) at  $-30$  °C. The reaction mixture was slowly warmed to ambient temperature and was stirred at 25 °C for 14 h. The solvent was evaporated to dryness yielding a pasty yellow solid, and then it was dissolved in pentane (30 mL) and the solution passed through an activated Celite pad. The yellow crystals of the title compound were grown from concentrated pentane solution at  $-30$  °C. Nucleation of crystal growth sometime starts on warming the pentane solution from  $-30$  °C to room temperature. Yield: 0.32 g (60%). Mp: 170–171 °C.  $^1\text{H}$  NMR (500 MHz,  $\text{C}_6\text{D}_6$ , 25 °C, TMS;  $\delta$ ):  $-0.53$  (s, 6H,  $\text{Al}-\text{CH}_3$ ); 1.17 (d, 12H,  $^3J_{\text{H}-\text{H}} = 6.8$  Hz,  $\text{CH}(\text{CH}_3)_2$ ); 1.19 (d, 12H,  $^3J_{\text{H}-\text{H}} = 6.8$  Hz,  $\text{CH}(\text{CH}_3)_2$ ); 1.29 (d, 12H,  $^3J_{\text{H}-\text{H}} = 6.8$  Hz,  $\text{CH}(\text{CH}_3)_2$ ); 1.31 (d, 12H,  $^3J_{\text{H}-\text{H}} = 6.8$  Hz,  $\text{CH}(\text{CH}_3)_2$ ); 1.52 (s, 12H,  $\text{CH}_3$ ); 2.84 (s, 12H,  $\text{Ti}-\text{N}(\text{CH}_3)_2$ ); 3.26 (sept., 4H,  $^3J_{\text{H}-\text{H}} = 6.8$  Hz,  $\text{CH}(\text{CH}_3)_2$ ); 3.63 (sept., 4H,  $^3J_{\text{H}-\text{H}} = 6.8$  Hz,  $\text{CH}(\text{CH}_3)_2$ ); 4.98 (s, 2H,  $\gamma\text{-CH}$ ); 7.06–7.22 (m, 12H, aryl protons).  $^{13}\text{C}$  NMR (125.75 MHz,  $\text{C}_6\text{D}_6$ , 25 °C, TMS;  $\delta$ ):  $-10.9$  (br s,  $\text{Al}-\text{CH}_3$ ); 23.9 (s,  $\text{CH}_3$ ); 24.7 (s,  $\text{CH}(\text{CH}_3)_2$ ); 26.5 (s,  $\text{CH}(\text{CH}_3)_2$ ); 28.1 (s,  $\text{CH}(\text{CH}_3)_2$ ); 28.6 (s,  $\text{CH}(\text{CH}_3)_2$ ); 46.1 (s,  $\text{Ti}-\text{N}(\text{CH}_3)_2$ ); 98.5 ( $\gamma\text{-CH}$ ); 124.4, 127.0, 141.9, 144.3, 144.7 (s, aryl carbon, *p*, *m*, *o*, and *i*, respectively); 170.2 (s, (CN)). MS (EI) [ $m/z$  (%): 1086.8 (4) [ $\text{M}]^+$ , 1071.8 (64) [ $\text{M} - \text{Me}]^+$ , 202 (100) [ $\text{DippNCCH}_3$ ] $^+$ . Anal. Calcd for  $\text{C}_{64}\text{H}_{100}\text{Al}_2\text{N}_6\text{O}_2\text{Ti}$ : C, 70.69; H, 9.26; N, 7.73. Found: C, 70.24; H, 9.25; N, 7.61.

**Synthesis of  $L(\text{Me})\text{Al}(\mu\text{-O})\text{Zr}(\text{NMe}_2)_2(\mu\text{-O})\text{Al}(\text{Me})\text{L}$  (**8**).** A solution of  $L(\text{Me})\text{Al}(\text{OH})$  (0.477 g, 1.0 mmol) in toluene (20 mL) was added dropwise by a syringe over a period of 15 min to a solution of  $\text{Zr}(\text{NMe}_2)_4$  (0.133 g, 0.50 mmol) in toluene (20 mL) at

$-30$  °C. The reaction mixture was slowly warmed to ambient temperature and was stirred at 25 °C for 14 h. The solvent was evaporated to dryness yielding a colorless solid, and then it was dissolved in *n*-hexane (40 mL) and the solution passed through an activated Celite pad. The resulting solution was concentrated to approximately 15 mL under reduced pressure and kept at 0 °C for several days yielding colorless crystals of analytical purity. Yield: 0.42 g (75%). Mp: 246–247 °C.  $^1\text{H}$  NMR (500 MHz,  $\text{C}_6\text{D}_6$ , 25 °C, TMS;  $\delta$ ):  $-0.58$  (s, 6H,  $\text{Al}-\text{CH}_3$ ); 1.12 (d, 12H,  $^3J_{\text{H}-\text{H}} = 6.8$  Hz,  $\text{CH}(\text{CH}_3)_2$ ); 1.18 (d, 12H,  $^3J_{\text{H}-\text{H}} = 6.8$  Hz,  $\text{CH}(\text{CH}_3)_2$ ); 1.29 (d, 12H,  $^3J_{\text{H}-\text{H}} = 6.8$  Hz,  $\text{CH}(\text{CH}_3)_2$ ); 1.33 (d, 12H,  $^3J_{\text{H}-\text{H}} = 6.8$  Hz,  $\text{CH}(\text{CH}_3)_2$ ); 1.52 (s, 12H,  $\text{CH}_3$ ); 2.81 (s, 12H,  $\text{Zr}-\text{N}(\text{CH}_3)_2$ ); 3.26 (sept., 4H,  $^3J_{\text{H}-\text{H}} = 6.8$  Hz,  $\text{CH}(\text{CH}_3)_2$ ); 3.56 (sept., 4H,  $^3J_{\text{H}-\text{H}} = 6.8$  Hz,  $\text{CH}(\text{CH}_3)_2$ ); 4.95 (s, 2H,  $\gamma\text{-CH}$ ); 7.06–7.24 (m, 12H, aryl protons).  $^{13}\text{C}$  NMR (125.75 MHz,  $\text{C}_6\text{D}_6$ , 25 °C, TMS;  $\delta$ ):  $-11.1$  (s,  $\text{Al}-\text{CH}_3$ ); 23.7 (s,  $\text{CH}_3$ ); 24.5 (s,  $\text{CH}(\text{CH}_3)_2$ ); 26.1 (s,  $\text{CH}(\text{CH}_3)_2$ ); 28.2 (s,  $\text{CH}(\text{CH}_3)_2$ ); 28.6 (s,  $\text{CH}(\text{CH}_3)_2$ ); 43.3 (s,  $\text{Zr}-\text{N}(\text{CH}_3)_2$ ); 98.1 ( $\gamma\text{-CH}$ ); 124.5, 127.0, 141.6, 144.1, 144.8, (s, aryl carbon, *p*, *m*, *o*, and *i*, respectively); 169.8 (s, (CN)). MS (EI) [ $m/z$  (%): 202 (100) [ $\text{DippNCCH}_3$ ] $^+$ . Anal. Calcd for  $\text{C}_{64}\text{H}_{100}\text{Al}_2\text{N}_6\text{O}_2\text{Zr}$ : C, 67.98; H, 8.91; N, 7.43. Found: C, 67.66; H, 9.00; N, 7.34.

**X-ray Structure Determination of **7** and **8**.** Suitable crystals of **7** and **8** were mounted on a glass fiber and data was collected on an IPDS II Stoe image-plate diffractometer (graphite-monochromated  $\text{Mo K}\alpha$  radiation,  $\lambda = 0.71073$  Å) at 133(2) K. The data was integrated with X-Area. The structures were solved by Direct Methods (SHELXS-97)<sup>19</sup> and refined by full-matrix least-squares methods against  $F^2$  (SHELXL-97).<sup>20</sup> All non-hydrogen atoms were refined with anisotropic displacement parameters. One of the eight isopropyl groups in both **7** and **8** was found to be disordered. The hydrogen atoms were refined isotropically on calculated positions using a riding model. Crystallographic data are presented in Table 1.

**Computational Details.** The calculations were performed at the well-established DFT level of theory making use of the B3LYP functional<sup>21,22</sup> as implemented in the Gaussian program package<sup>23</sup> employing a basis-set termed LANL2DZ<sup>24</sup> for Ti and 6-31G<sup>25,26</sup> for the remaining atoms. In the first step the compound was fully optimized to its equilibrium structure. The resulting electronic wave function for the structure was then analyzed to obtain the shape of the molecular orbitals, and a NBO analysis<sup>27–29</sup> was performed to ascertain the bonding situation.

**Polymerization of Ethylene.** The polymerization reactions were carried out on a high-vacuum line ( $10^{-5}$  Torr) in an autoclave (Buchi). In a typical experiment, 100 mL of dry toluene (from Na/K) was vacuum-transferred into the polymerization flask and saturated with 1.0 atm of rigorously purified ethylene. The catalyst (10  $\mu\text{mol}$ ) was taken in the Schlenk flask, and appropriate MAO (1.6 M in toluene, Witco GmbH) was added. The mixture was

(19) Sheldrick, G. M. *Acta Crystallogr., Sect. A* **1990**, *46*, 467–473.

(20) Sheldrick, G. M. *SHELXL-97*; University of Göttingen: Göttingen, Germany, 1997.

(21) Lee, C.; Yang, W.; Parr, R. G. *Phys. Rev. B* **1988**, *37*, 785–789.

(22) Miehlisch, B.; Savin, A.; Stoll, H.; Preuss, H. *Chem. Phys. Lett.* **1989**, *157*, 200–206.

(23) Frisch, M. J.; et al. *Gaussian 03*, revision C.02; Gaussian, Inc.: Wallingford, CT, 2004 (see Supporting Information).

(24) Hay, P. J.; Wadt, W. R. *J. Chem. Phys.* **1985**, *82*, 270–283.

(25) Petersen, G. A.; Al-Laham, M. A. *J. Chem. Phys.* **1991**, *94*, 6081–6090.

(26) Petersen, G. A.; Bennett, A.; Tensfeldt, T. G.; Al-Laham, M. A.; Shirley, W. A.; Mantzaris, J. *J. Chem. Phys.* **1988**, *89*, 2193–2218.

(27) Foster, J. P.; Weinhold, F. *J. Am. Chem. Soc.* **1980**, *102*, 7211–7218.

(28) Reed, A. E.; Weinhold, F. *J. Chem. Phys.* **1985**, *83*, 1736–1740.

(29) Reed, A. E.; Curtiss, L. A.; Weinhold, F. *Chem. Rev.* **1988**, *88*, 899–926.

stirred for 20 min to activate the catalyst. The catalyst solution was then quickly injected into the rapidly stirred flask using a gastight syringe. After a measured time interval, the polymerization was quenched by the addition of methanol (5 mL), and the reaction mixture was then poured into methanol (800 mL). The polymer was allowed to fully precipitate overnight and then collected by filtration, washed with fresh methanol, and dried.

**Acknowledgment.** This work is supported by the Göttinger Akademie der Wissenschaften, Deutsche Forschungsgemeinschaft, and the Fonds der Chemischen Industrie.

S.K.M thanks the Alexander von Humboldt Foundation for a research fellowship.

**Supporting Information Available:** Complete ref 23, X-ray data for **7** and **8** (CIF), and tables of crystallographic and structural refinement data, atomic coordinates, bond lengths, bond angles, anisotropic thermal parameters, and calculated atomic coordinates of **7** and **8** (PDF). This material is available free of charge via the Internet at <http://pubs.acs.org>.

IC701063V